Nikhil Navkar (Orcid ID: 0000-0003-1853-1910)

Evaluation of User-Interfaces for Controlling Movements of Virtual Minimally Invasive Surgical Instruments

Dehlela Shabir [a], Malek Anbatawi [a], Jhasketan Padhan [a], Shidin Balakrishnan [a], Abdulla Al-Ansari [a], Julien Abinahed [a], Panagiotis Tsiamyrtzis [b], Elias Yaacoub [c], Amr Mohammed [c], Zhigang Deng [d], Nikhil V. Navkar [a,*]

[a] Department of Surgery, Hamad Medical Corporation, Doha, Qatar
[b] Department of Mechanical Engineering, Politecnico di Milano, Milan, Italy
[c] Department of Computer Science and Engineering, Qatar University, Doha, Qatar
[d] Department of Computer Science, University of Houston, Houston, Texas, USA

Corresponding Author
Department of Surgery, Surgical Research Section
Hamad General Hospital, Hamad Medical Corporation, Doha, Qatar. PO Box 3050
E-mail Address: nnavkar@hamad.qa
Phone: +974 7760 – 6674

Category: Original Article
Manuscript word count: ~4,000

CONFLICT OF INTEREST

The authors of this submission have NO affiliations with or involvement in any organization or entity with any financial interest (such as honoraria; educational grants; participation in speakers' bureaus; membership, employment, consultancies, stock ownership, or other equity interest; and expert testimony or patent-licensing arrangements), or non-financial interest (such as personal or professional relationships, affiliations, knowledge or beliefs) in the subject matter or materials discussed in this manuscript.

ETHICS

The ethical committee (Medical Research Center, Qatar) at the Hamad Medical Corporation approved the study.

AUTHORS CONTRIBUTION

D. Shabir and N.V. Navkar led the study and manuscript writing. M. Anbatawi and J. Padhan assisted in testing of the user-interfaces and data collection. S. Balakrishnan, A. Al-Ansari and J. Abinahed provided input from the surgical point-of-view to the manuscript. E. Yaacoub and A. Mohammed assisted in the computer networking and provided revisions of the manuscript. Z. Deng provided input in the human computer interfacing and provided revisions of the manuscript. P. Tsiamyrtzis performed the statistical analysis of the data.

DATA AVAILABILITY STATEMENT

Research data not sharable.

Abstract

Background: Recent tele-mentoring technologies for minimally invasive surgery (MIS) augments the operative field with movements of virtual surgical instruments as visual cues. The objective of this work is to assess different user-interfaces that effectively transfer mentor's hand gestures to the movements of virtual surgical instruments.

Methods: A user study was conducted to assess three different user-interface devices (Oculus-Rift, SpaceMouse, Touch Haptic device) under various scenarios. The devices were integrated with a MIS tele-mentoring framework for control of both manual and robotic virtual surgical instruments.

Results: The user study revealed that Oculus Rift is preferred during robotic scenarios, whereas the touch haptic device is more suitable during manual scenarios for tele-mentoring.

Conclusion: A user-interface device in the form of a stylus controlled by fingers for pointing in 3D space is more suitable for manual MIS, whereas a user-interface that can be moved and oriented easily in 3D space by wrist motion is more suitable for robotic MIS.

KEYWORDS: Minimally invasive surgery, Tele-mentoring, User-interfaces, Virtual surgical instruments, Surgical simulations

Introduction

Tele-medicine is playing an ever-increasing role in clinical practice with the aim to provide clinical healthcare from a distance [1,2]. It entails the use of software/hardware technologies to share clinical information and edit its content in real-time. An aspect of tele-medicine, when applied to surgical context, includes tele-mentoring and tele-collaboration during a surgery [3-5]. Augmented reality based enabling technologies have been developed to facilitate tele-mentoring between an operating and a remote surgeon during a minimally invasive surgery (MIS). It involves the use of user interfaces that assist the mentor (the remote surgeon) to perform screen markings [6-8] or display augmented hands gestures [9-11] to the mentee (the operating surgeon). More sophisticated user interfaces allow the mentor to transfer realistic visual cues in a form of the motion of virtual surgical instruments and has emerged as an effective mode of transferring information pertaining to tool-tissue interaction [12-15]. The surgical instruments used for MIS are articulated in nature with multiple degrees-of-freedom and exhibit movement in three-dimensional (3D) space with constraints imposed by incision points [16]. To control these virtual surgical instruments, high degrees-of-freedom (DOF) input devices are generally needed to accurately capture human hand movement from the real world and translate it to the movement of virtual surgical instruments overlaid onto the operative field. Thus, a suitable user-friendly input device is necessary to facilitate efficient acquisition of information that the mentor wants to convey to the mentee.

In a MIS tele-mentoring, the mentor demonstrates the required tool-tissue interaction to the mentee using virtual surgical instrument motions. The mentee mentally grasps these visual cues (augmented on the operating field) and performs the surgical sub-step as demonstrated by the mentor. The study performed by Shabir et al. [17] shows that a path (projected on a two-dimensional operative field) defined by the mentor's virtual surgical instrument movement when compared to a predefined path varies with Dynamic Time Warping (DTW) distance of 1176.5 ± 331.8. DTW distance is a similarity measure between two paths [18] and is used to assess the similarity between the paths defined by motions of surgical instruments [19,20]. In the operating room, when the mentee replicates the motion of virtual instrument performed by the mentor, the average DTW distance further increases to 3195.3 ± 971.4 between the paths defined by the mentor's instrument movements and those of the mentee. Therefore, a selection of suitable of user interface is vital to reduce the prior error that may be induced in the tele-mentoring system by the mentor while manipulating virtual surgical instrument using the user interface. This will ensure that the information rendered to the mentee is accurate from the mentor's side.

Several previous works have been done to study and compare user interfaces for tele-robotic surgery and tele-mentoring scenarios during MIS [21-23]. These studies included quantification of human-machine interactions via user-interfaces for tele-robotic surgery[21], comparison of user interfaces of robotic surgical platforms based on degrees-of-freedom and force feedback [22], and perception and interpretation of the transmitted operating field video on different visualization interfaces for tele-mentoring [23]. Though, the notion of using a user interface to control virtual surgical instrument motion for tele-mentoring has been explored and demonstrated in both laparoscopic [12,13,17,24] and robotic surgery [13-15,17], why a particular user interface was empirically chosen to use in previous tele-mentoring studies is not reasoned. Considering the variety of existing off-the-shelf user interface systems, it is a priority to compare, understand, and quantify the effectiveness, efficiency, and usability of such different user interfaces for tele-mentoring applications in MIS. Indeed, to best of our

knowledge, no previous studies have evaluated and compared different user interfaces for tele-mentoring in MIS. In particular, to evaluate whether the user interfaces enable the mentor to demonstrate accurately and in timely manner the motion of the virtual surgical instrument along a path required for interacting with the tissue. Table 1 depict such different user-interfaces used in tele-mentoring systems for MIS.

It is imperative to understand and quantify the effectiveness and efficiency of various user-interfaces in different scenarios before incorporating them with a surgical tele-mentoring system. The objective of this work is to compare and evaluate user interface devices in terms of their efficiencies in controlling the motion of virtual surgical instruments during a minimally invasive surgical tele-mentoring scenario. Three standard off-the-shelf user interface devices are chosen, and an interfacing algorithm is developed to process the input from these interface devices and convert it to the motion of virtual laparoscopic as well as robotic surgical instruments augmented on the operative field. An experimental study is conducted to evaluate the user interface devices for effectively transferring the mentor's hand gestures to the movements of virtual surgical instruments required in tele-mentoring.

Materials and Methods

To evaluate the user interfaces for surgical tele-mentoring during a MIS, a tele-mentoring framework proposed by Shabir et al. [13,17] was used for the experiments in our study. The setup at the mentee's site (representing the operating room) captures the position of the incision points, the orientation and position of the scope, and the video feed acquired from the scope camera (representing the view of the operating field). This information is transferred over a network from the mentee's site to the mentor's site and is rendered on a visualization screen. Virtual surgical instruments are overlaid onto the view of the operating field (acquired from the scope) such that it appears as if the instruments are inserted through the incision points. The movements of virtual surgical instruments are controlled by the user interfaces. Three different user interface devices were chosen and integrated with the setup at the mentor's site. The interfaces are described in subsection I. The interfacing algorithm developed for rendering the motion of a virtual surgical instrument, which is controlled by the interfaces, is presented in subsection II. Finally, the details of the user study are explained in subsection III.

I. Interface Devices Used in the Study

Three interfaces were used in the study (as shown in Figure 1): (a) Oculus Rift – Meta (formerly Facebook), (b) SpaceMouse – 3Dconnexion, and (c) Touch Haptic Device – 3D Systems. The three devices were chosen as they provide 6 DOFs inputs (three translations and three rotations) and can be purchased off-the-shelf. In the study, simulation of the virtual robotic surgical instrument requires 6 DOFs input, whereas the virtual laparoscopic surgical instrument required only 4 DOFs input. Compared to the SpaceMouse, both the Oculus Rift (a lightweight hand controller that moves in 3D space) and the Touch Haptic Device (in form of a hand-held stylus that moves in 3D space) require calibration. A clutch system was implemented for Oculus Rift and Touch Haptic interfaces. As the interfaces provide absolute poses (i.e. positions and orientations), the clutch system enables ergonomic repositioning of the styluses (or controllers) of the user-interfaces. The SpaceMouse interface provides incremental poses, and as a result no calibration is required; neither a clutch system was

implemented during the study. The mapping of the laparoscopic and robotic tooltip motion with the motion of the interface's stylus is presented in Figure 2. From a cost perspective, the SpaceMouse and Oculus Rift cost less (in range of $300-$700) as compared to the Touch Haptic Device (over $1000). The higher cost of Touch Haptic Device is due to the motors used for rendering feedback forces in the virtual environment. In the study, no feedback forces were rendered using the Touch Haptic Device.

II. Interfacing Algorithm

The following Algorithm-1 *RenderInstrument* describes the rendering of the overlaid virtual surgical instrument motion controlled by the user interface device, during our experiments.

Algorithm-1 *RenderInstrument* renders the motion of a virtual surgical instrument controlled by the interface
Input: $toolType, interfaceType, M_{World}^{Scope}(t), M_{Scope}^{Interface}, x_{Incision}$
1: Set $M_{World}^{EndEffector}(t)$ in front of scope camera frame $M_{World}^{Scope}(t)$,
2: $M_{World}^{EndEffector}(t_0) \leftarrow M_{World}^{EndEffector}(t)$
3: **if** (*interfaceType* doesn't uses clutch)
4:      $M_{Interface}^{Stylus}(t_0) \leftarrow M_{Identity}$
5:      $\emptyset(t_0) \leftarrow 0$
6: **end if**
7: **while** (*augmentationRequired*) **do**
8:      Get $M_{Interface}^{Stylus}(t), \emptyset(t),$ and *clutch* state from the interface
9:      **if** (*interfaceType* uses clutch **and** *clutch* is turned ON from OFF state)
10:          $M_{Interface}^{Stylus}(t_0) \leftarrow M_{Interface}^{Stylus}(t)$
11:          $M_{World}^{EndEffector}(t_0) \leftarrow M_{World}^{EndEffector}(t)$
12:          $\emptyset(t_0) \leftarrow \emptyset(t)$
13:      **end if**
14:      **if** (*interfaceType* uses clutch **and** *clutch* is in ON state) **or** (*interfaceType* doesn't uses clutch)
15:          $M_{World}^{Stylus}(t) \leftarrow M_{World}^{Scope}(t) . M_{Scope}^{Interface} . M_{Interface}^{Stylus}(t)$
16:          $M_{World}^{Stylus}(t_0) \leftarrow M_{World}^{Scope}(t) . M_{Scope}^{Interface} . M_{Interface}^{Stylus}(t_0)$
17:          Compute $\delta_{Translation}(t)$ between frames $M_{World}^{Stylus}(t)$ and $M_{World}^{Stylus}(t_0)$
18:          **if** (*toolType* is robotic)
19:              Compute $\delta_{Rotation}(t)$ between frames $M_{World}^{Stylus}(t)$ and $M_{World}^{Stylus}(t_0)$
20:              Compute $M_\delta(t)$ from $\delta_{Rotation}(t)$ and $\delta_{Translation}(t)$
21:              $M_{World}^{EndEffector}(t) \leftarrow M_\delta(t) M_{World}^{EndEffector}(t_0)$
22:          **end if**
23:          **if** (*toolType* is laparoscopic)
24:              Compute $M_\delta(t)$ from $\delta_{Translation}(t)$
25:              $M_{World}^{EndEffector}(t) \leftarrow M_\delta(t) M_{World}^{EndEffector}(t_0)$
26:              $M_{World}^{EndEffector}(t) \leftarrow reorient (M_{World}^{EndEffector}(t), M_{World}^{EndEffector}(t_0), x_{Incision}, \emptyset(t), \emptyset(t_0))$
27:          **end if**
28:      **end if**
29:      **if** (*interfaceType* doesn't uses clutch)
30:          $M_{World}^{EndEffector}(t_0) \leftarrow M_{World}^{EndEffector}(t)$
31:      **end if**
32:      Compute *DoFs* based on *tooltype*, $x_{Incision}$, and $M_{World}^{EndEffector}(t)$
33:      Apply *DoFs* to render the *tooltype*
34: **end while**

The above algorithm *RenderTool* renders the motion of a virtual surgical instrument overlaid onto the operative field. The inputs of this algorithm include: *tooltype* (which can be a robotic or laparoscopic), *interfaceType* (to detect whether it uses clutch), the incision point $x_{Incision}(t)$,

$\text{M}_{\text{World}}^{\text{Scope}}(t)$ frame representing the pose of the surgical scope camera with respect to the world (Figure 3a), and $\text{M}_{\text{Scope}}^{\text{Interface}}(t)$ frame representing the mapping of the interface workspace with respect to scope. The pose of the stylus within the interface workspace is represented by frame $\text{M}_{\text{Interface}}^{\text{Stylus}}(t)$. The interface controls the pose of an end effector frame $\text{M}_{\text{World}}^{\text{EndEffector}}(t)$, which represents the pose of the tooltip (Figure 3b). Clutch is used to ergonomically reposition the stylus of the interface. When the clutch is in the OFF state, the operator can reposition the stylus without moving the virtual instrument. When the clutch is turned ON from the OFF state, the stylus frame $\text{M}_{\text{Interface}}^{\text{Stylus}}(t_0)$, rotation angle $\emptyset(t_0)$ (in the case of laparoscopic instrument), and current end effector frame $\text{M}_{\text{World}}^{\text{EndEffector}}(t_0)$ are recorded. Any subsequent relative movement of the stylus represented by $M_\delta(t)$ is computed and applied to the end effector frame $\text{M}_{\text{World}}^{\text{EndEffector}}(t_0)$ to obtain the current end effector frame $\text{M}_{\text{World}}^{\text{EndEffector}}(t)$.

The end effector frame $\text{M}_{\text{World}}^{\text{EndEffector}}(t)$ is reoriented for laparoscopic instrument type. This is to ensure the constraints imposed by a limited degree-of-freedom laparoscopic instrument are included while computing $\text{M}_{\text{World}}^{\text{EndEffector}}(t)$. The $x_{\text{EndEffector}}(t)$ is set to the origin of $\text{M}_{\text{World}}^{\text{EndEffector}}(t)$ frame and $\mu(t_0)$ to the Z-Axis of $\text{M}_{\text{World}}^{\text{EndEffector}}(t)$ frame. A new frame is computed with $x_{\text{EndEffector}}(t)$ as the origin and axes reoriented. The X-Axis is set to $(x_{\text{EndEffector}}(t) - x_{\text{Incision}}(t))$. The Y-Axis is computed as the cross product of $\mu(t_0)$ and $(x_{\text{EndEffector}}(t) - x_{\text{Incision}}(t))$. The Y axis is then rotated along $(x_{\text{EndEffector}}(t) - x_{\text{Incision}}(t))$ by an angle $\emptyset(t) - \emptyset(t_0)$. The Z axis is set to be orthogonal to both X and Y axes.

Algorithm-1 computes the degrees-of-freedom required for rendering the virtual surgical instrument. In the case of robotic instrument type, a four degree-of-freedom surgical instrument is used with each DOF represented by joint angles $\theta_1, \theta_2, \theta_3,$ and θ_4 (Figure 3c) and positions of each joint represented by vectors $x_1, x_2,$ and x_3 (Figure 3d). The x_3 and x_0 are set to $x_{\text{EndEffector}}(t)$ and $x_{\text{Incision}}(t)$. A frame is defined with the origin x_3, X-axis n_x coincides with the X-axis of $\text{M}_{\text{World}}^{\text{EndEffector}}(t)$, the Z-axis n_z is orthogonal to both n_x and vector $x_3 - x_0$, and Y-axis n_Y is orthogonal to both n_x and n_z. x_2 is computed as $x_3 + \lambda_{23} n_Y$, where λ_{23} denotes the distance between x_2 and x_3. x_1 is computed as $x_2 + \lambda_{12}(x_0 - x_2)/\|(x_0 - x_2)\|$, where λ_{12} denotes the distance between x_1 and x_2. θ_2 is computed as the angle substituted by vectors $(x_3 - x_2)$ with $(x_2 - x_1)$. A unit vector $n_{\text{Orthogonal}}$ is defined orthogonal to both $x_0 - x_2$ and n_{UpVector}. θ_1 is computed as the angle substituted by vectors $n_z \times (x_0 - x_2)$ with $n_{\text{Orthogonal}}$. θ_3 is computed as the angle substituted between n_z and Z-axis of $\text{M}_{\text{World}}^{\text{EndEffector}}(t)$. θ_4 corresponds to the opening and closing of the tooltips contributing to the pinching mechanism, and the tooltips are rendered at $\theta_3 + \theta_4$ and $\theta_3 - \theta_4$. In the case of laparoscopic instrument type, a two degree-of-freedom surgical instrument (Figure 3e) is used. It is considered as a special case of four degree-of-freedom robotic instrument type, where θ_3 and θ_2 are constant (180 degrees).

III. Setup for the User Study

Six participants (right-handed with the ages from 26 to 35 years old) from the Department of Surgery at Hamad General Hospital, Doha, Qatar participated in the user study. The participant are researchers (non-surgeons) with expertise in developing surgical technologies and have previously experienced virtual and mixed reality environments. The study was approved by the institutional review board comprising of the ethical committee (Medical Research Center, Doha, Qatar, approval number MRC-01-20-087). The inclusion criteria were set to include participants who have previous experience in maneuvering laparoscopic

and robotic (da Vinci Xi – Intuitive surgical Inc.) surgical instruments. Before the study, the participants went through a 10 to 15 minutes preparatory session to get familiar with the controls of the three user interfaces for maneuvering the virtual surgical instruments. The preparatory session was completed for each participant after the participant was able to map the input from the user interfaces to the translation and rotation motion of the virtual surgical instruments (as depicted in Figure 2). The participants then took part in simulated scenarios as mentors. The scenarios involved assessing the motion of virtual laparoscopic and robotic surgical instruments along a path using the user interfaces (Figure 4a).

For the study, four surgical scenarios, namely A, B, C, and D, were simulated. The details of each scenario are presented in Table 2. Laparoscopic tooltips have fewer degrees-of-freedom as compared to robotic tooltips, resulting in limited articulation. This constraint was taken into consideration while designing the scenarios. The scenarios A, B, and C were designed to enable comparison of the interfaces for both the laparoscopic and robotic tooltips. In each of the simulated scenarios A, B, and C, the participants performed three trials. The order of usage of the three user interfaces in our study was randomized for each participant (using a simple randomization [25]). Once a particular user interface was selected, the combination of tool-type (laparoscopic or robotic) and scenario (A, B, or C) were also randomized for the trials. Robotic tools with a higher articulation enable the participants to orient the tooltips. To evaluate the interfaces for this particular feature, scenario D was designed. In the case of scenario D (Figure 4b), only one trial was conducted. The factorial aspect of the experiment lead to 57 trials for each participant. The priority was to increase the robustness of estimations by having three trials per subject for each scenario. Though it limited the total number of participants to only six, it gave a more robust estimation of performance measures.

During the study, the input provided by the participants via the user interfaces for maneuvering the virtual surgical tooltips were recorded. The recoded input and the corresponding motion of the overlaid virtual tooltips were processed to extract meaningful indices (presented in Table 3) for measuring the performance. T-tests were used to determine if there is a significant difference between the means of the recorded indices among different scenarios. The t-tests were selected as the collected data are continuous random variables (for both duration and distance metrics). Furthermore, the assumptions (over the normality and homogeneity of variance) regarding the t-tests were carefully examined and validated.

Results

Figure 5 and Figure 6 compare the average durations to complete the task for scenarios A (right hand only), B (left hand only), and C (using both hands), using the three different user interfaces. In the case of laparoscopic surgical instruments (Figure 5), if the mentor needs to demonstrate the motion of a single virtual surgical instrument using either the right or the left hand only (i.e., in scenario A or B), all the three user interfaces take the same duration. However, when the mentor needs to demonstrate tool-tissue interaction using both hands (scenario C), the SpaceMouse takes significantly more time (42 ± 16 seconds), compared to Oculus Rift (31 ± 8 seconds, $p = 0.009$) and Touch Haptic device (31 ± 16 seconds, $p = 0.03$). In the case of robotic surgical instruments (Figure 6), the SpaceMouse requires more time to complete the task, compared to Oculus Rift and Touch Haptic device in all the three scenarios A, B, and C. Furthermore, for robotic surgical instruments in scenario C, the Touch

Haptic device takes less time (23 ± 8 seconds, p < 0.02), compared to the time taken by Oculus Rift (33 ± 11 seconds).

Figure 5 and Figure 6 also compare the average distances maintained by the tooltip during the tasks. For laparoscopic surgical instruments in scenario A (Figure 5), using the three interfaces is equivalent to traversing the path. However, in the case of scenario B, the SpaceMouse deviates further (11.65 ± 6.99 millimeters) as compared to both Oculus Rift (5.50 ± 1.23 millimeters, p = 0.0004) and Touch Haptic device (5.36 ± 0.89 millimeters, p = 0.0003). Also, in the scenario C, the SpaceMouse deviates more (12.08 ± 3.80 millimeters) than both Oculus Rift (10.04 ± 4.10 millimeters, p = 0.05) and Touch Haptic device (11.04 ± 5.01 millimeters, p = 0.06). This shows SpaceMouse is effective in tele-mentoring when a single virtual instrument motion needs to be displayed and the motion is controlled by the mentor's dominant hand (which is the right-hand in the case of this study). In the case of robotic surgical instruments (Figure 6), the participants were able to traverse the path with a better accuracy (smaller deviations) using Oculus Rift, compared to other two interfaces in all the three scenarios.

In Figure 7, the participants performed better using Oculus Rift for the movements of robotic virtual surgical instruments, compared to their manual counterpart. Though it takes similar time to complete the task, the average distance maintained by the tooltip from the path during the task is smaller for robotic virtual surgical instruments than the manual counterpart in all the three scenarios A, B, and C. In the case of Touch Haptic device, no significant difference was found between manipulating robotic or manual virtual surgical instruments. In the case of SpaceMouse, the participants performed better for the movements of manual virtual surgical instruments than for those of robotic virtual surgical instruments. It takes shorter time (in scenario A and B) as well as the virtual instrument tooltip deviates less from the path (in all the three scenarios).

During a minimally invasive surgical tele-mentoring sub-step, the mentor needs to demonstrate to the mentee a series of tooltip movements over a period. During these movements (such as suturing or cauterization) the tooltip of the virtual surgical instrument should stay on a pre-defined path with respect to the nearby tissues. To compare the user interfaces on this aspect, distribution of the percentages of time spent in a bin was used. While the aforementioned results presented in Figure 5, Figure 6, and Figure 7 compare the user interfaces on the basis of two metrics (the average duration to complete the task and the average distance maintained by the tooltip from the path during the task), Figure 8 combines the two metrics into one. It illustrates a comparison of the percentages of time spent in the four bins (with sizes varying from 0 to 5 mm, 5 to 10 mm, 10 to 15 mm, and greater than 15 mm) by the virtual surgical instrument's tooltip controlled via different user interfaces across scenarios A, B, and C during the task. Similar to a histogram, the distribution of the time percentages spent in a bin (Table 3) facilitates to analyze and compare the proximity of the tooltip from the path during the task. Greater percentage of time is spent in lower distance bins (such as 0 to 5 mm), the closer the tooltip movement to the predefined path during the task. In the case of laparoscopic (manual) surgical instruments, Touch Haptic device takes precedence over SpaceMouse in terms of maintaining a higher accuracy as a user interface for the mentor. No significant difference was found between Touch Haptic device and Oculus Rift. In contrast, for robotic surgical instruments, Oculus Rift showed a higher accuracy for a larger percentage of duration, compared to both Touch Haptic device and SpaceMouse. Another interesting pattern, which can be observed in Figure 8, is that Oculus Rift performs

similarly in both scenarios A (right hand is only used) and B (left hand is only used). One reasonable explanation could be that the control of the virtual surgical instruments in the case of Oculus Rift is performed by wrist motion rather than finger movements (as in the case of both Touch Haptic device and SpaceMouse).

Figure 9 shows the time required to orient the tooltip of a robotic surgical instrument to match the rendered V-shape. We observe that Oculus Rift takes less time as compared to SpaceMouse while traversing the path left to right and vice versa.

Discussion

In summary, during a tele-mentoring for minimally invasive robotic surgical applications, when both the mentor and the mentee have comparable surgical macro-skills (such as maneuvering of surgical instruments, general expertise in anatomy, ability to distinguish surrounding anatomical structures, and assess tissue thickness [17]), the Touch Haptic Device is more suitable to demonstrate the motion of virtual surgical instrument overlaid onto the surgical field. The Touch Haptic Device assists the mentor to traverse a pre-defined path faster (especially for scenarios A and C with robotic tooltips). However, when the mentee has not perfected the surgically relevant micro-skills (such as economy of movement, visual tactility, and tool-tissue interaction [26,27]), more accurate virtual surgical instrument motion needs to be depicted. In such a case, Oculus Rift as a user interface device is more preferred as it assists the mentor to traverse a pre-defined path with lesser deviation (as observed in all the three scenarios for robotic tooltips).

On the other hand, for tele-mentoring of minimally invasive laparoscopic (manual) surgery, uses of the Touch Haptic Device and Oculus Rift are approximately equivalent for maneuvering the virtual surgical instruments. A laparoscopic virtual surgical instrument uses 4 DOFs input: 3 for translations and 1 for rotation. Translating the tooltip is sufficient to position the entire virtual laparoscopic surgical instrument with respect to the operative field during a tele-mentoring task and is easily doable using Touch Haptic Device and Oculus Rift. Due to this, both the devices performed equivalently across the three scenarios. The rotation of the virtual laparoscopic surgical instrument along its shaft assists the mentor to demonstrate the orientation of the tooltip for surgical tasks, such as cutting, cauterization, or grasping. For the mentee, the information can be perceived by analyzing the pose of the virtual instrument with respect to the tissue being operated. In such cases, a user interface that facilitates translations of the tooltip in the 3D space is sufficient for laparoscopic (manual) tele-mentoring.

A minimally invasive tele-mentoring system may be used for both laparoscopic as well as robotic surgery [13,17]. In such a case, the Touch Haptic Device may be suitable as it performs equivalently for both types of surgery. The choice of the user interface for tele-mentoring may also depend upon other aspects, such as cost and size. The mentor may be present at a site where a proper MIS tele-mentoring hardware is not installed. In such a case, a portable user-interface could be connected to a laptop with an Internet connection as a remote tele-mentoring setup. Though the Touch Haptic device is a suitable user interface device for both laparoscopic and robotic surgical instrument manipulation, the cost and size may be limiting factors for its usage at the mentor site. On similar grounds, though the Oculus Rift which satisfies both aspects of low cost and portability, it requires calibration and may be tedious to

set up at the mentor's site. Therefore, in scenarios where all the three user interface devices perform similarly, SpaceMouse can be a preferred choice due to its low cost and compact portable size (for example, in Scenario A of laparoscopic virtual surgical instrument control).

While the user study was tailored to assess the user interfaces for MIS tele-mentoring scenarios, future work would be geared towards assessing the user interfaces on three broader directions. The first direction would be to explore its applicability for open surgeries, where mixed reality [28] or augment reality [29] can be used to overlay virtual surgical instruments movement on the operating field. As the motion of the instruments are not constrained (in contrast to MIS), the results of the current user study cannot be extrapolated and would require conducting user studies for tele-mentoring scenarios in open surgeries. The second direction could be surgical simulations where an operator interacts with a computer-generated virtual environment of the operating field [30]. The user interfaces can be adapted to replicate the controllers present on the console of robotic surgical systems. A comparative user study would identify the user interfaces suitable for interacting the virtual environment [31,32]. The third direction could be preoperative surgical planning in a mixed reality environment [33,34]. For interfacing with mixed reality environment, user studies have shown that hand gestures may not be a suitable mode for sending instructions and a suitable user-interface is required [35,36].

Conclusion

The presented user study compares three off-the-shelf user interface devices in terms of their effectiveness when used to manipulate virtual surgical instruments overlaid onto the operative field during tele-mentoring. Both the Oculus Rift and the Touch Haptic device are preferred over SpaceMouse to demonstrate tool-tissue interactions in tele-mentoring scenarios. However, SpaceMouse is more suitable for positing virtual surgical instruments as a pointing device.

References

1. Mahar JH, Rosencrance JG, Rasmussen PA. Telemedicine: Past, present, and future. *Cleve Clin J Med*. Dec 2018;85(12):938-942. doi:10.3949/ccjm.85a.17062

2. Ponsky TA, Schwachter M, Parry J, Rothenberg S, Augestad KM. Telementoring: the surgical tool of the future. *Eur J Pediatr Surg*. Aug 2014;24(4):287-94. doi:10.1055/s-0034-1386646

3. Asiri A, AlBishi S, AlMadani W, ElMetwally A, Househ M. The Use of Telemedicine in Surgical Care: a Systematic Review. *Acta Inform Med*. Oct 2018;26(3):201-206. doi:10.5455/aim.2018.26.201-206

4. El-Sabawi B, Magee W. The evolution of surgical telementoring: current applications and future directions. *Ann Transl Med*. Oct 2016;4(20):391. doi:10.21037/atm.2016.10.04

5. Schlachta CM, Nguyen NT, Ponsky T, Dunkin B. Project 6 Summit: SAGES telementoring initiative. *Surg Endosc*. 09 2016;30(9):3665-72. doi:10.1007/s00464-016-4988-5

6. Bruns NE, Irtan S, Rothenberg SS, Bogen EM, Kotobi H, Ponsky TA. Trans-Atlantic Telementoring with Pediatric Surgeons: Technical Considerations and Lessons Learned. *J Laparoendosc Adv Surg Tech A*. Jan 2016;26(1):75-8. doi:10.1089/lap.2015.0131

7. Nguyen NT, Okrainec A, Anvari M, et al. Sleeve gastrectomy telementoring: a SAGES multi-institutional quality improvement initiative. *Surg Endosc*. Feb 2018;32(2):682-687. doi:10.1007/s00464-017-5721-8

8. Agarwal R, Levinson AW, Allaf M, Makarov D, Nason A, Su LM. The RoboConsultant: telementoring and remote presence in the operating room during minimally invasive urologic surgeries using a novel mobile robotic interface. *Urology*. Nov 2007;70(5):970-4. doi:10.1016/j.urology.2007.09.053

9. Webpage. Proximie. Accessed 31st December, 2018. https://www.proximie.com/

10. Andersen D, Popescu V, Cabrera ME, et al. An Augmented Reality-Based Approach for Surgical Telementoring in Austere Environments. *Mil Med*. 03 2017;182(S1):310-315. doi:10.7205/MILMED-D-16-00051

11. Davis MC, Can DD, Pindrik J, Rocque BG, Johnston JM. Virtual Interactive Presence in Global Surgical Education: International Collaboration Through Augmented Reality. *World Neurosurg*. Feb 2016;86:103-11. doi:10.1016/j.wneu.2015.08.053

12. Vera AM, Russo M, Mohsin A, Tsuda S. Augmented reality telementoring (ART) platform: a randomized controlled trial to assess the efficacy of a new surgical education technology. *Surg Endosc*. Dec 2014;28(12):3467-72. doi:10.1007/s00464-014-3625-4

13. Shabir D, Abdurahiman N, Padhan J, et al. Towards Development of a Tele-Mentoring Framework for Minimally Invasive Surgeries. *International Journal of Medical Robotics and Computer Assisted Surgery*. 2021;

14. Jarc AM, Shah SH, Adebar T, et al. Beyond 2D telestration: an evaluation of novel proctoring tools for robot-assisted minimally invasive surgery. *J Robot Surg*. Jun 2016;10(2):103-9. doi:10.1007/s11701-016-0564-1

15. Jarc AM, Stanley AA, Clifford T, Gill IS, Hung AJ. Proctors exploit three-dimensional ghost tools during clinical-like training scenarios: a preliminary study. *World J Urol*. Jun 2017;35(6):957-965. doi:10.1007/s00345-016-1944-x

16. Anderson PL, Lathrop RA, Webster RJ. Robot-like dexterity without computers and motors: a review of hand-held laparoscopic instruments with wrist-like tip articulation. *Expert Rev Med Devices*. 07 2016;13(7):661-72. doi:10.1586/17434440.2016.1146585

17. Shabir D, Abdurahiman N, Padhan J, et al. Preliminary design and evaluation of a remote tele-mentoring system for minimally invasive surgery. *Surg Endosc*. Mar 04 2022;doi:10.1007/s00464-022-09164-3

18. Sakoe H, Chiba S. Dynamic Programming Algorithm Optimization for Spoken Word Recognition. *IEEE Transactions on Acoustics, Speech, and Signal Processing*. 1978;ASSP-26(1):43-49.

19. Despinoy F, Bouget D, Forestier G, et al. Unsupervised Trajectory Segmentation for Surgical Gesture Recognition in Robotic Training. *IEEE Trans Biomed Eng*. 06 2016;63(6):1280-91. doi:10.1109/TBME.2015.2493100

20. Despinoy F, Zemiti N, Forestier G, Sánchez A, Jannin P, Poignet P. Evaluation of contactless human-machine interface for robotic surgical training. *Int J Comput Assist Radiol Surg*. Jan 2018;13(1):13-24. doi:10.1007/s11548-017-1666-6

21. Hoshyarmanesh H, Zareinia K, Lama S, Durante B, Sutherland GR. Evaluation of haptic devices and end-users: Novel performance metrics in tele-robotic microsurgery. *Int J Med Robot*. Aug 2020;16(4):e2101. doi:10.1002/rcs.2101

22. Simorov A, Otte RS, Kopietz CM, Oleynikov D. Review of surgical robotics user interface: what is the best way to control robotic surgery? *Surg Endosc*. Aug 2012;26(8):2117-25. doi:10.1007/s00464-012-2182-y

23. Budrionis A, Hartvigsen G, Lindsetmo RO, Bellika JG. What device should be used for telementoring? Randomized controlled trial. *Int J Med Inform*. Sep 2015;84(9):715-23. doi:10.1016/j.ijmedinf.2015.05.004

24. Lowry B, Johnson GGRJ, Vergis A. Merged virtual reality teaching of the fundamentals of laparoscopic surgery: a randomized controlled trial. *Surg Endosc*. Jan 03 2022;doi:10.1007/s00464-021-08939-4

25. Suresh K. An overview of randomization techniques: An unbiased assessment of outcome in clinical research. *J Hum Reprod Sci*. Jan 2011;4(1):8-11. doi:10.4103/0974-1208.82352

26. Clevin L, Grantcharov TP. Does box model training improve surgical dexterity and economy of movement during virtual reality laparoscopy? A randomised trial. *Acta Obstet Gynecol Scand*. 2008;87(1):99-103. doi:10.1080/00016340701789929

27. Sánchez A, Rodríguez O, Sánchez R, et al. Laparoscopic surgery skills evaluation: analysis based on accelerometers. *Jsls*. Oct-Dec 2014;18(4)doi:10.4293/jsls.2014.00234

28. Gasques D, Johnson JG, Sharkey T, et al. ARTEMIS: A Collaborative Mixed-Reality System for Immersive Surgical Telementoring. *Proceedings of the 2021 CHI Conference on Human Factors in Computing Systems*. 2021;

29. Rojas-Muñoz E, Cabrera ME, Andersen D, et al. Surgical Telementoring Without Encumbrance: A Comparative Study of See-through Augmented Reality-based Approaches. *Ann Surg*. 08 2019;270(2):384-389. doi:10.1097/SLA.0000000000002764

30. Moglia A, Ferrari V, Morelli L, Ferrari M, Mosca F, Cuschieri A. A Systematic Review of Virtual Reality Simulators for Robot-assisted Surgery. *Eur Urol*. 06 2016;69(6):1065-80. doi:10.1016/j.eururo.2015.09.021

31. Tanaka A, Graddy C, Simpson K, Perez M, Truong M, Smith R. Robotic surgery simulation validity and usability comparative analysis. *Surg Endosc*. 09 2016;30(9):3720-9. doi:10.1007/s00464-015-4667-y

32. Smith R, Truong M, Perez M. Comparative analysis of the functionality of simulators of the da Vinci surgical robot. *Surg Endosc*. Apr 2015;29(4):972-83. doi:10.1007/s00464-014-3748-7

33. Cristina M. Morales Mojica   JDVG, Nikhil V. Navkar , Shidin Balakrishnan , Julien Abinahed , Walid El Ansari , Khalid Al-Rumaihi , Adham Darweesh , Abdulla Al-Ansari , Mohamed Gharib , Mansour karkoub , Ernst L. Leiss , Ioannis Seimenis , Nikolaos V. Tsekos. A Prototype Holographic Augmented Reality Interface for Image-Guided Prostate Cancer Interventions. presented at: Eurographics Workshop on Visual Computing for Biology and Medicine; 2018;

34. Morales Mojica CM, Navkar NV, Tsekos NV, et al. Holographic Interface for three-dimensional Visualization of MRI on HoloLens: A Prototype Platform for MRI Guided Neurosurgeries. 2017:21-27.

35. Velazco-Garcia JD, Navkar NV, Balakrishnan S, et al. Evaluation of how users interface with holographic augmented reality surgical scenes: Interactive planning MR-Guided prostate biopsies. *Int J Med Robot*. Oct 2021;17(5):e2290. doi:10.1002/rcs.2290

36. Velazco-Garcia JD, Navkar NV, Balakrishnan S, et al. End-user evaluation of software-generated intervention planning environment for transrectal magnetic resonance-guided prostate biopsies. *Int J Med Robot*. Feb 2021;17(1):1-12. doi:10.1002/rcs.2179

TABLES

Table 1: User interfaces used in minimally invasive surgical tele-mentoring

Study	Surgery type	User interface	Minimally invasive surgical tele-mentoring scenario
Lowry et al. [24]	Laparoscopic (manual)	Laparoscopic tool	HelpLightning system was used to segment laparoscopic tool from the view of a box trainer at mentor's site and overlaid onto the mentee view. The tele-mentoring was used for assessment of FLS skills.
Vera et al. [12]	Laparoscopic (manual)	Laparoscopic tool	Similar to HelpLightning system, an augmented reality tele-mentoring (ART) platform was used for teaching intracorporeal suturing task.
Shabir et al. [13,17]	Laparoscopic (manual)	SpaceMouse	SpaceMouse was used to control the motion of laparoscopic instruments to assess the tele-mentoring between mentor and mentee.
Shabir et al. [13,17]	Robotic	Touch Haptic Device	Touch Haptic Device was used to control the motion of virtual robotic instruments to assess the tele-mentoring between mentor and mentee.
Jarc et al. [14]	Robotic	Razer™ Hydra - Sixense	Razer Hydra user interface was used to control motion of 3D virtual model of da Vinci Endowrist® large needle driver for dry-lab tasks that targeted basic technical skills.
Jarc et al. [15]	Robotic	Custom interface	A custom interface resembling da Vinci hand controller was used to control virtual model of Endowrist® instruments for tissue dissection and suturing in a live porcine model

Table 2: Surgical scenarios simulated in the user study

Simulated scenario	Tool types used	Participant's hand controlling the interface	Task performed by the participant in the scenario
Scenario A	Laparoscopic (manual) and robotic	Only right hand was used	Participant was asked to move the virtual surgical instrument along a path using right hand (Figure 4a). The task measured the ease of using the interface with right hand.
Scenario B	Laparoscopic (manual) and robotic	Only left hand was used	Participant was asked to move the virtual surgical instrument along a path using left hand. The task measured the ease of using the interface with left hand.
Scenario C	Laparoscopic (manual) and robotic	Both left and right hand were used concurrently	Participant was asked to move two virtual surgical instruments together along a path using both left and right hand. The task measured the ease of using the interface for dexterous maneuvering of the virtual surgical instruments using both hands.
Scenario D	Robotic	Both left and right hand were used consecutively	Participant was asked to orient a virtual surgical instrument (by matching it to a rendered V-shape as shown in Figure 4b) along a path while traversing. The tool was first traversed in a direction using right hand and then traversed back in the opposite direction using left hand.

Table 3: Indices used to compare performance of user interfaces during the user study

Indices	Description	Used in scenario			
		A	B	C	D
Total duration	The total time taken by a participant to complete the task.	✓	✓	✓	✓
Average distance	Average distance maintained by the tool from the path, i.e. summation of distance of the tooltip from the curve with respect to time divided by the total time to complete the task. $$d_{Average} = \frac{\sum \Delta t_i\, d_i}{\sum \Delta t_i}$$ Where Δt_i is the change in time for a given instance i and d_i is the Euclidian distance between the tooltip and the point on the path closest to the tooltip's position.	✓	✓	✓	
Percentage of time spent in a bin	Four bins with incremental size were defined (0-5, 5-10, 10-15, 15<). Each bin represents a range of distance maintained by the tooltip of the virtual surgical instrument from the path. The time spent in a bin corresponds to the time spent by the tooltip within the range of distance defined for the bin. The summation of the individual times in each bin gives the total duration. The percentage of the time spent in a bin is equal to the time spent in a bin with respect to the total duration.	✓	✓	✓	
Orientation Time	Time required to orient the tooltip to match the rendered V-Shape. The next V-shape along the path is rendered only when the user properly orients the virtual tooltip for the current V-shape.				✓

FIGURES
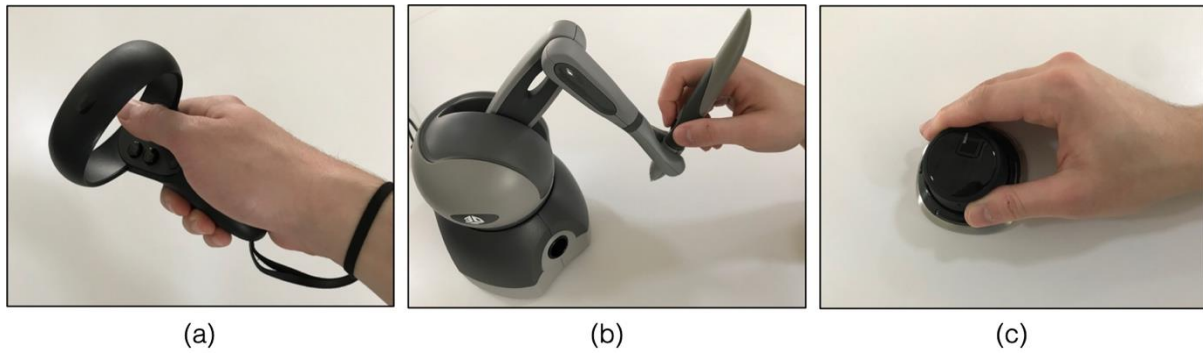
Figure 1: User interface devices used in the study: (a) Oculus Rift – Meta (formerly Facebook), (b) Touch Haptic Device – 3D Systems, and (c) SpaceMouse – 3Dconnexion
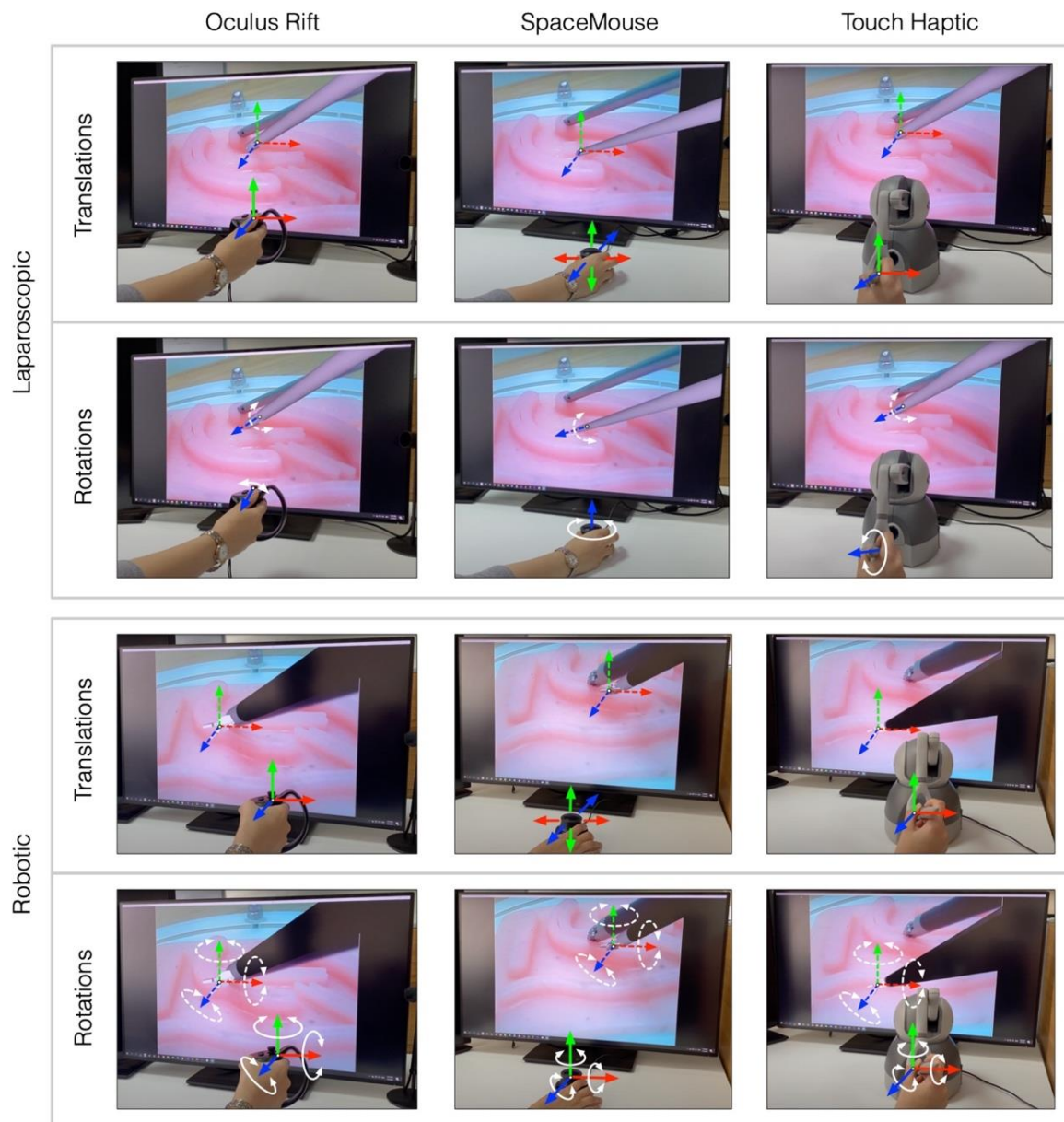
Figure 2: Mapping of the rotations and translations for the virtual laparoscopic and robotic tooltip motion with the motion performed by the stylus of the interfaces. Three interfaces were used, namely Oculus Rift, SpaceMouse, and Touch Haptic device. The mapping for robotic tooltips involved 3 degree-of-freedom for translation and 3 degree-of-freedom for rotation. The mapping for laparoscopic tooltip involved 3 degree-of-freedom for translation and 1 degree-of-freedom for rotation. Both real surgical instrument controlled by mentee and virtual surgical instrument controlled by mentor can be seen in the operative field.
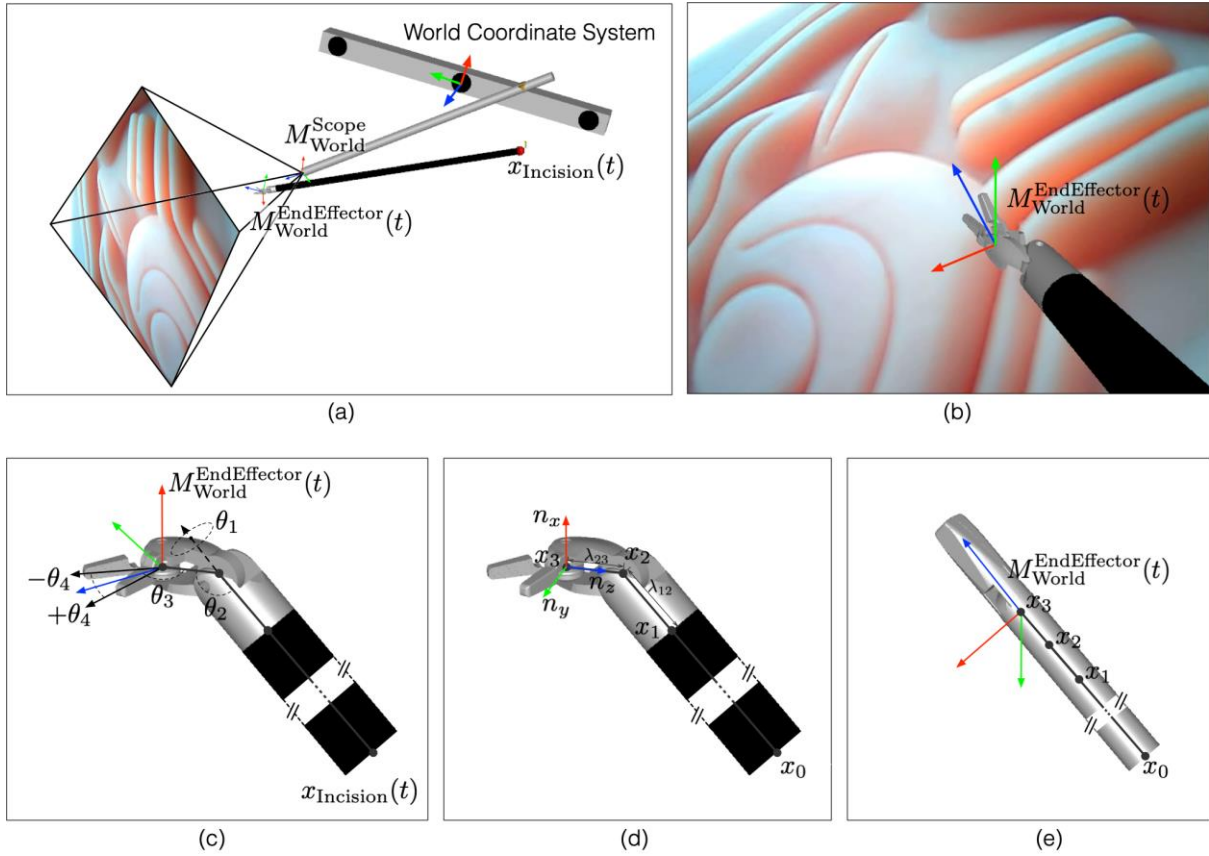
Figure 3: (a) Augmented reality environment, (b) end effector frame representing the pose of the tooltip, (c) joint angles for each degree-of-freedom for robotic tool, (d) positions of each joints for robotic tool, (e) positions of each joints for laparoscopic tool.
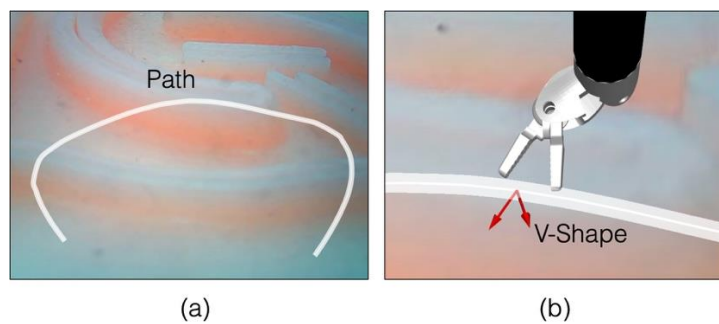
Figure 4: (a) Path rendered in Scenario A, B, and C (b) V-Shape rendered in Scenario D.
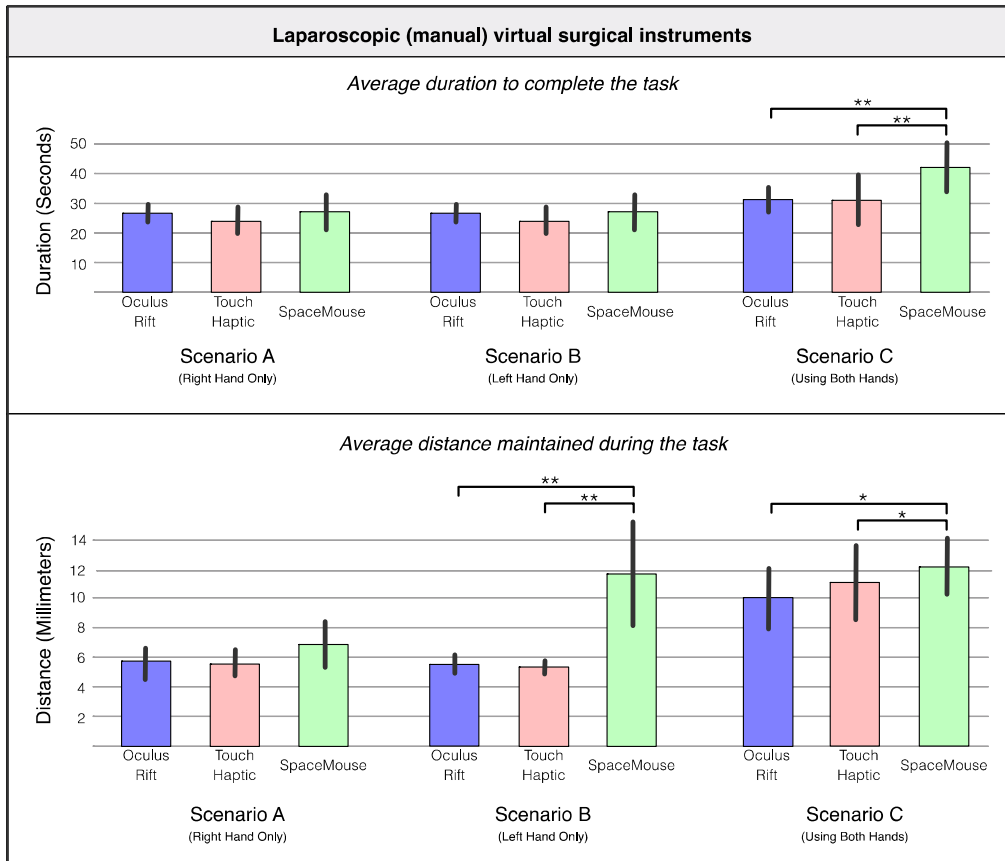
Figure 5: The average duration to complete the task and the average distance maintained by the tooltip during the task using the three user-interfaces for scenario A (right hand only), B (left hand only), and C (using both hands) in case of laparoscopic (manual) virtual surgical instruments. The comparison is tagged based on the p-value using a star-type categorization: if p-value ≤ 0.05 then '**', if $0.05 <$ p-value ≤ 0.1 then '*', and if $0.1 <$ p-value, then ' '.
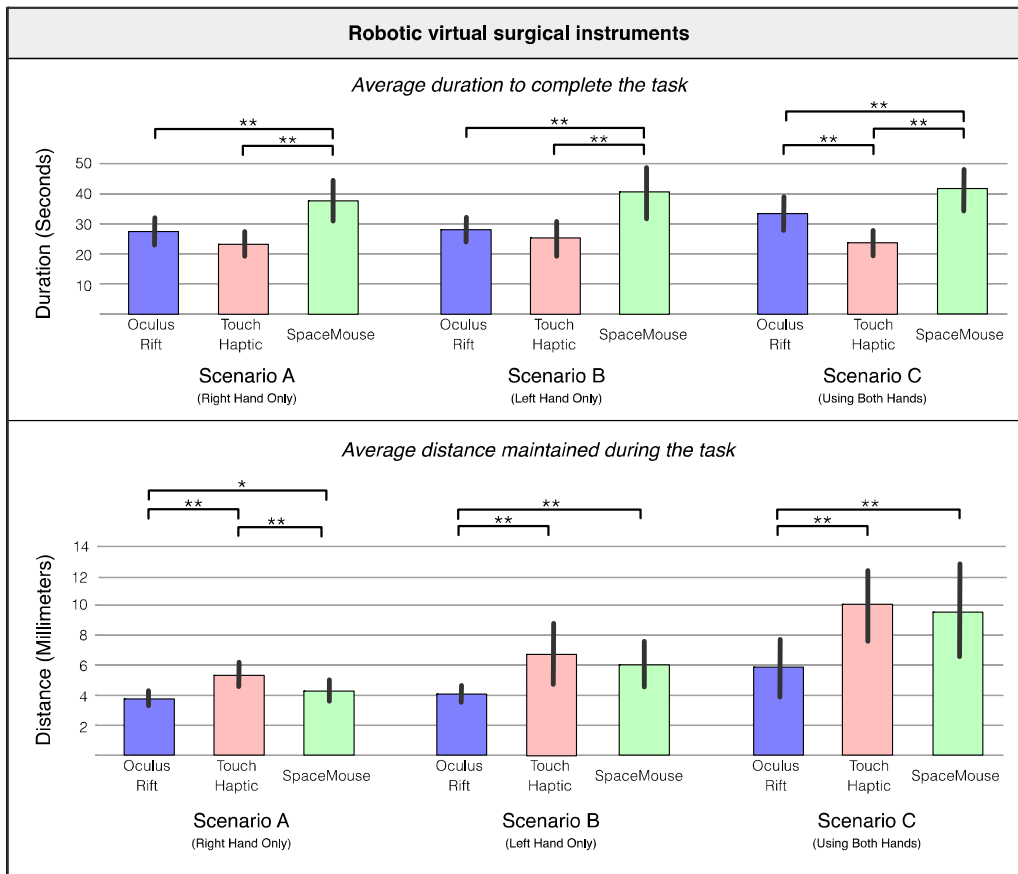
Figure 6: The average duration to complete the task and the average distance maintained by the tooltip during the task using the three user-interfaces for scenario A (right hand only), B (left hand only), and C (using both hands) in case of robotic virtual surgical instruments. The comparison is tagged based on the p-value using a star-type categorization: if p-value ≤ 0.05 then '**', if $0.05 <$ p-value ≤ 0.1 then '*', and if $0.1 <$ p-value, then ' '.
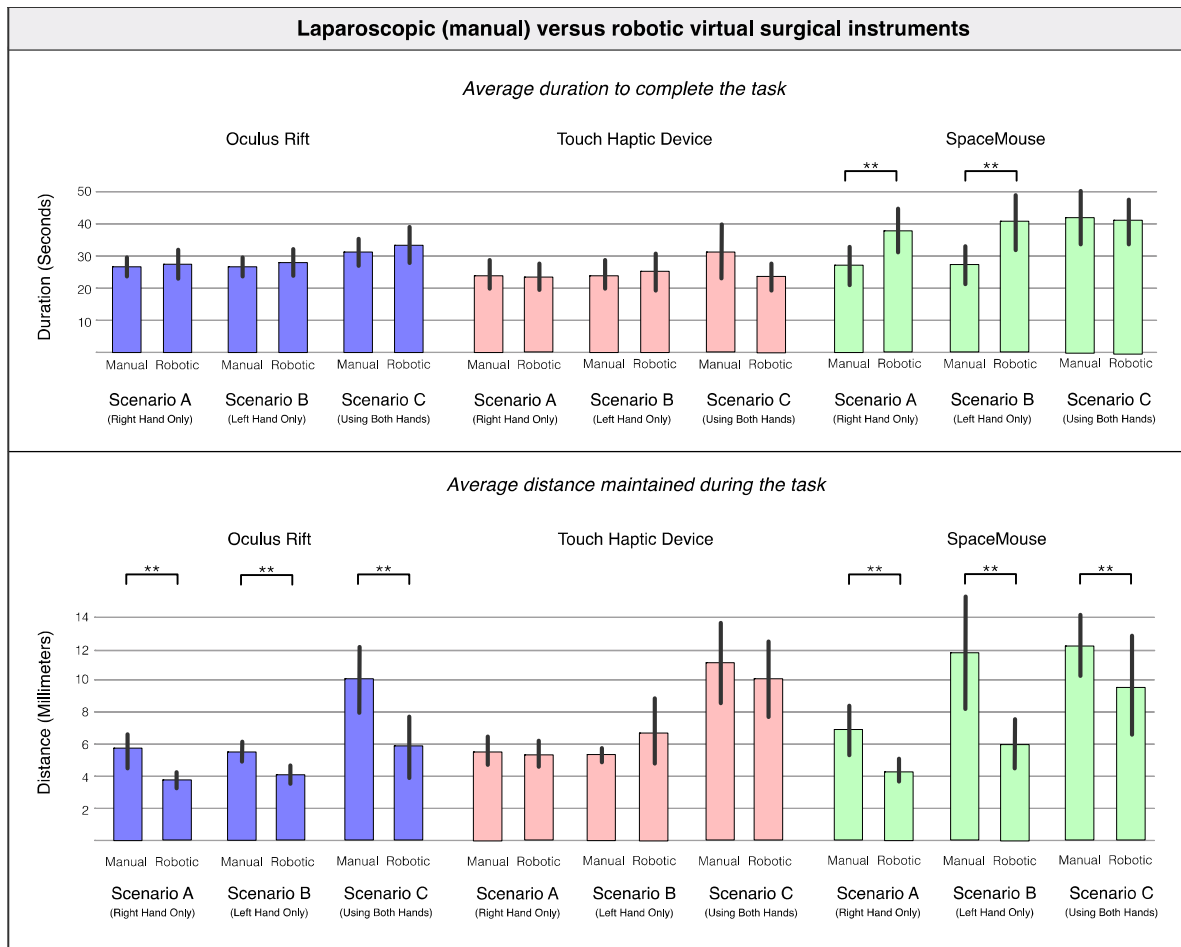
Figure 7: Comparison of the average duration to complete the task and the average distance maintained by the tooltip during the task for manual and robotic virtual surgical instruments. The comparison is tagged based on the p-value using a star-type categorization: if p-value $\leq$ 0.05 then '**', if $0.05 <$ p-value ≤ 0.1 then '*', and if $0.1 <$ p-value, then ' '.
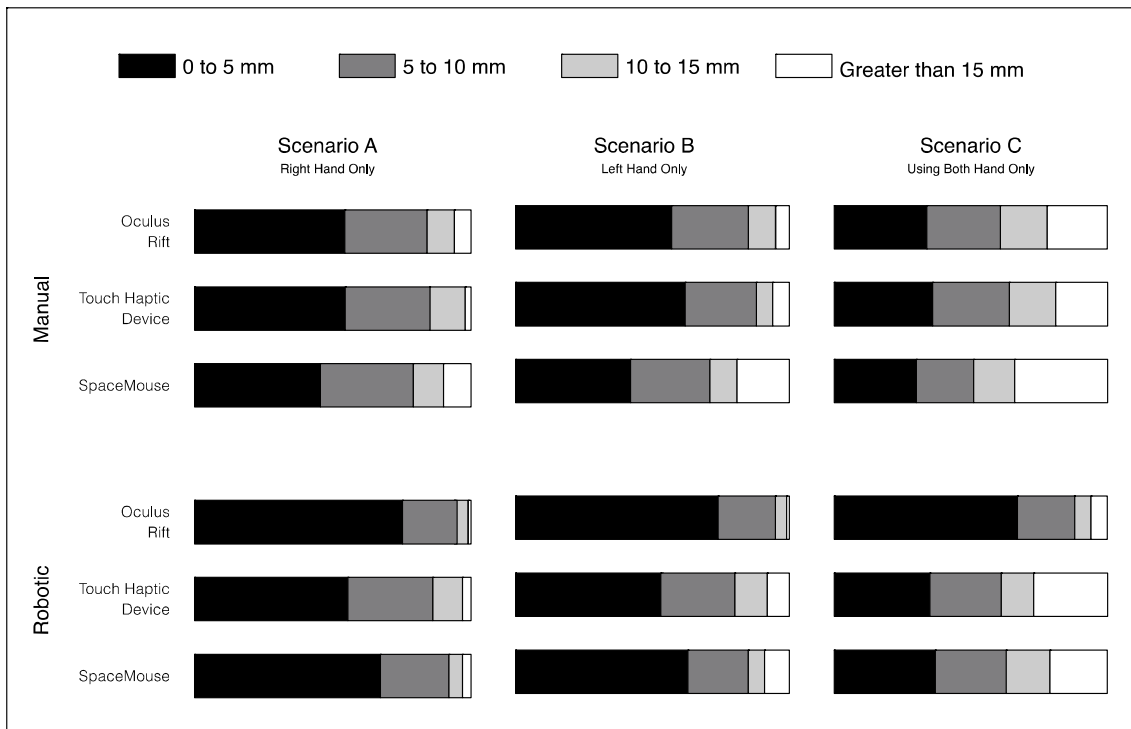
Figure 8: Percentage of time spent by the virtual surgical instrument in the four bins with incremental size varying from 0 to 5 mm, 5 to 10 mm, 10 to 15 mm, and greater than 15 mm. Each bin represents a range of distances. The shortest distance between the tooltip of the virtual surgical instrument from the path is computed and categorized into one of the four bins. A percentage of time spent in a bin is calculated as the time spent by the tooltip in a given range of distance (corresponding to a bin) with respect to the total duration of the task.

Robotic virtual surgical instruments

Average duration to complete the orientation task
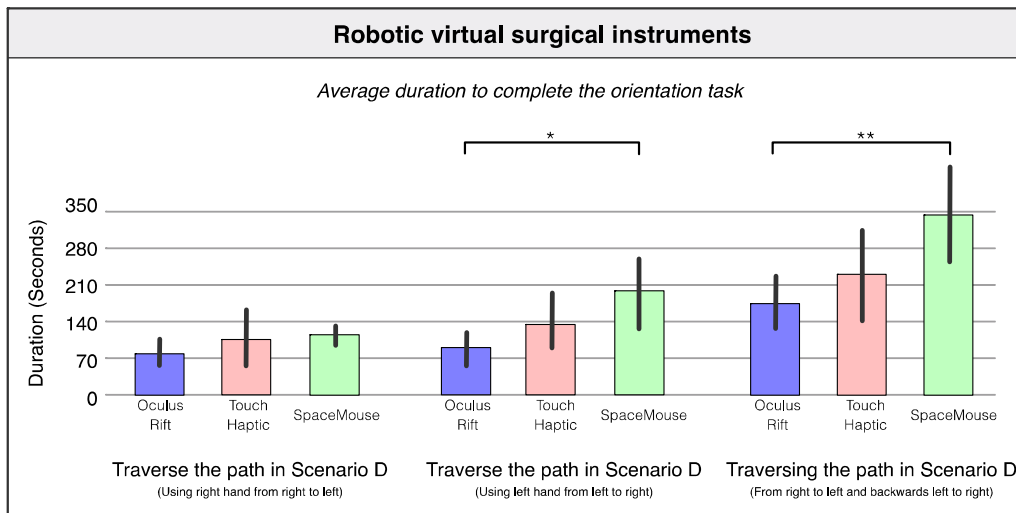
Figure 9: Comparison of average orientation time taken by each interface in scenario D when using robotic tools. The comparison is tagged based on the p-value using a star-type categorization: if p-value ≤ 0.05 then '**', if 0.05 < p-value ≤ 0.1 then '*', and if 0.1 < p-value, then ' '.

Appendix

In this appendix, we provide the detailed check of assumptions for all the t-tests performed in the manuscript. Precisely, for all the T-tests in Figures 5, 6, 7 and 9 (using the numbering adopted in the revised manuscript) we will examine if the basic assumptions needed for the T-tests are violated or not. Specifically, we will examine the normality assumption of each sample and whether the two groups examined in each t-test violate the assumption of equal variances or not (i.e. homogeneity of variance assumption).

To examine the normality assumption we will provide the normal probability plot of each group (NPP from now on), which is a QQ-plot of the sample against the theoretic quantiles of the standard normal distribution and we will also add the theoretic line, which connects the first and third quartiles of the standard normal distribution (denoted with red color in the plots). Proximity of the points to the red line (i.e. linear relationship in the plot) will indicate normality. Apart from the visual inspection of the points though we will perform a statistical test to examine the normality assumption. Precisely, we will perform the "Anderson-Darling test" along with the "Wilk-Shapiro test" that examine the conformance of each sample with the normal distribution. Precisely, for each subpanel of a Figure we will present the NPP and we will add as legend to the plot the p-values of the two tests performed (A.D.pv = Anderson-Darling p-value and W.S.pv = Wilk-Shapiro p-value).

For the naming of the plots in Figures 5, 6 and 7, the rule is: X_Y_Z_W, where

X = **L** for Laparoscopic or **R** for Robotic

Y = Device with **O** for Oculus Rift, **T** for Touch Haptic or **S** for Space Mouse

Z = Scenario with **A**, **B** or **C**.

W = Metric used with **dur** for duration or **dist** for distance

In Figure 9 where the scenario is D, the notation of Z changes to:

Z = Hand used with **R** for Right, **L** for Left or **T** for Total.

For the homogeneity of variance we will examine in every test of whether the participating samples have the same variance or not using the "Levene test".

In all the tests described above (i.e. both for normality and homogeneity of variance) p-values that are very small will indicate violation of assumptions. The cutoff value α (i.e. level of significance) against which we will compare the p-values is typically considered to be a small number like 0.01 or 0.05.

Figure 5 DURATION
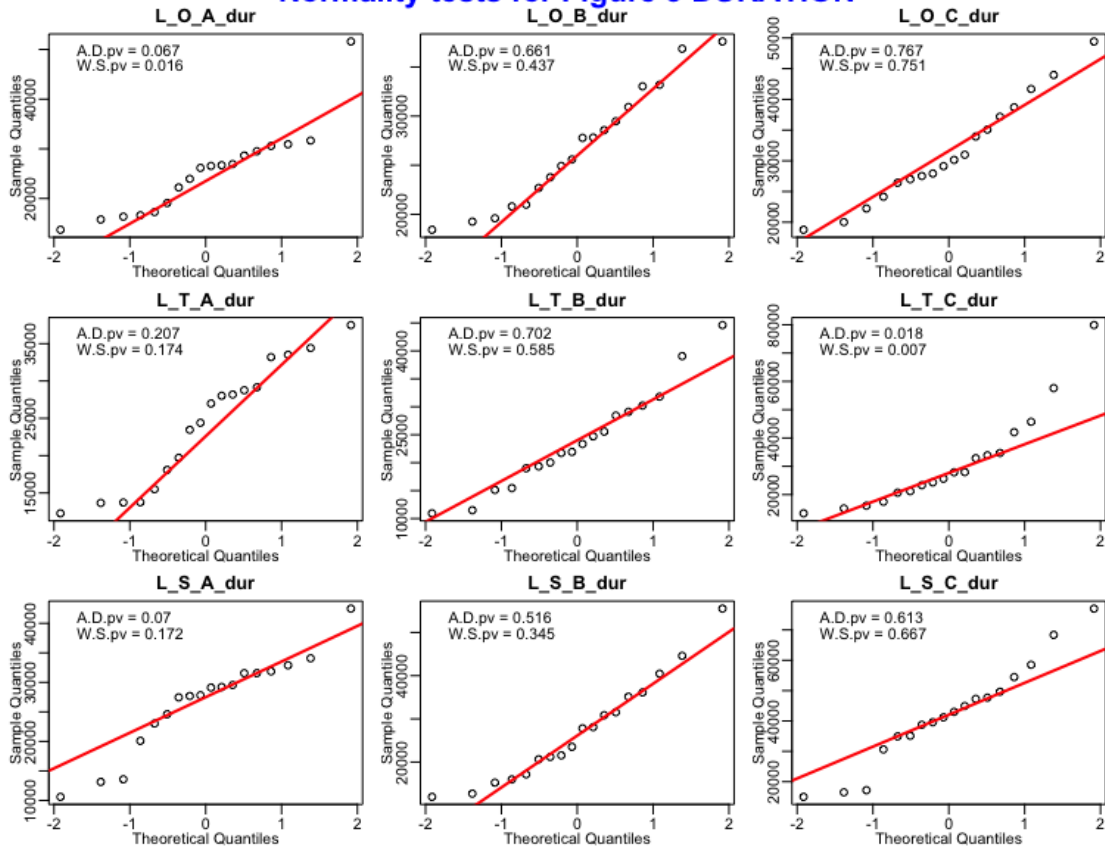
LAPAROSCOPIC		Levene's test p-value
Scenario A Duration	Oculus Rift vs Touch Haptic	0.682
	Oculus Rift vs Space Mouse	0.833
	Touch Haptic vs Space Mouse	0.500
Scenario B Duration	Oculus Rift vs Touch Haptic	0.248
	Oculus Rift vs Space Mouse	0.018
	Touch Haptic vs Space Mouse	0.216
Scenario C Duration	Oculus Rift vs Touch Haptic	0.147
	Oculus Rift vs Space Mouse	0.049
	Touch Haptic vs Space Mouse	0.815

Figure 5 DISTANCE

Normality tests for Figure 5 DISTANCE
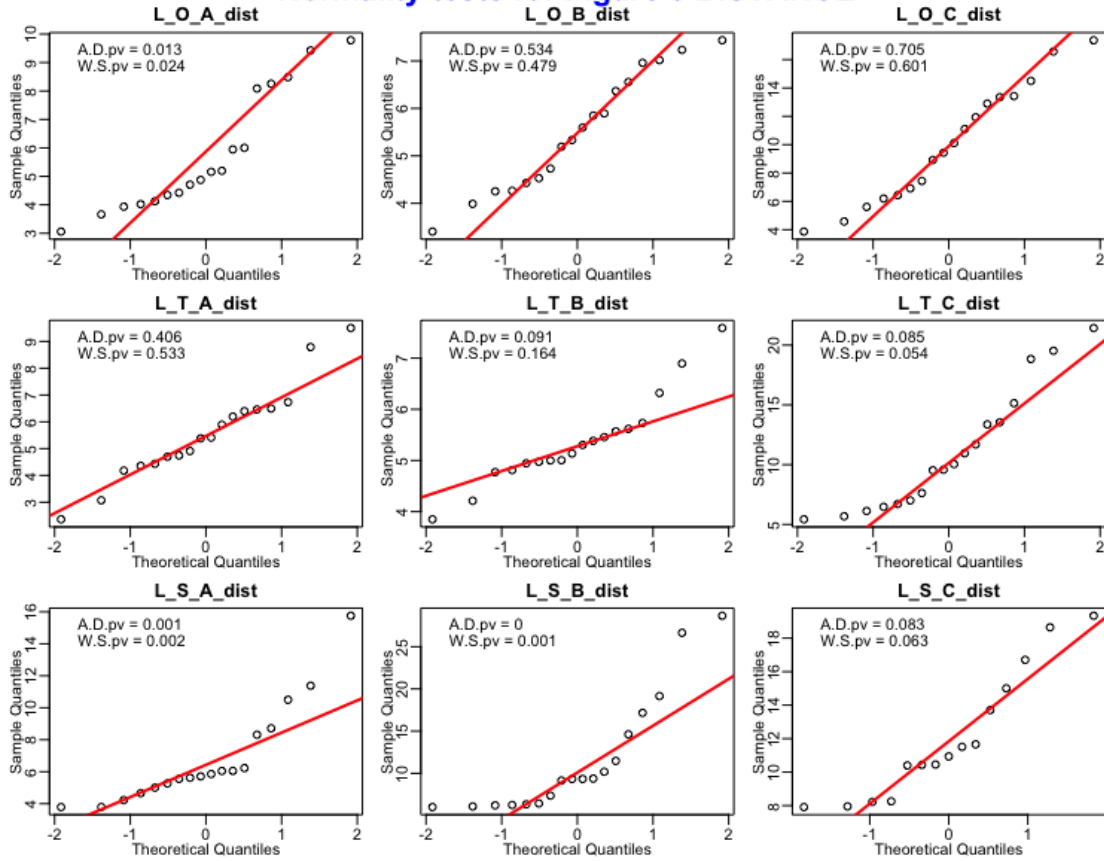
LAPAROSCOPIC		Levene's test p-value
Scenario A Distance	Oculus Rift vs Touch Haptic	0.501
	Oculus Rift vs Space Mouse	0.636
	Touch Haptic vs Space Mouse	0.343
Scenario B Distance	Oculus Rift vs Touch Haptic	0.049
	Oculus Rift vs Space Mouse	0.011
	Touch Haptic vs Space Mouse	0.005
Scenario C Distance	Oculus Rift vs Touch Haptic	0.607
	Oculus Rift vs Space Mouse	0.490
	Touch Haptic vs Space Mouse	0.325

Figure 6 DURATION
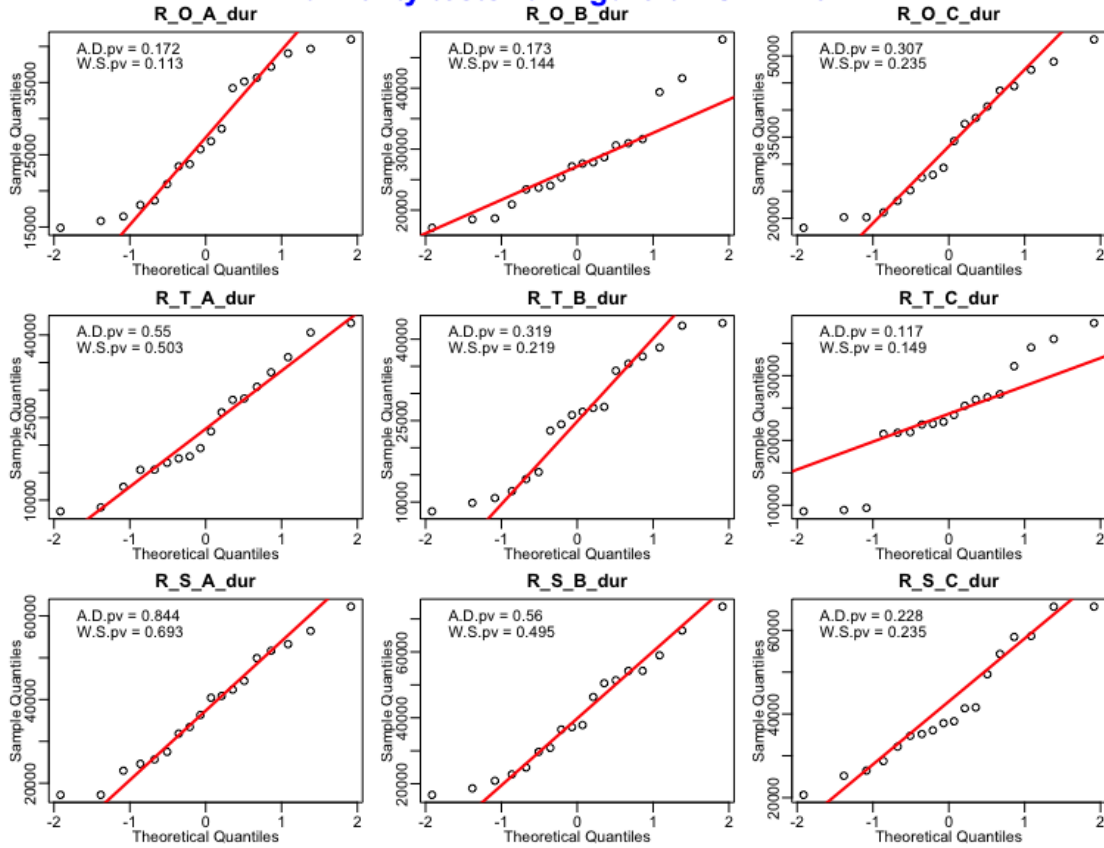
ROBOTIC			Levene's test p-value
Scenario A Duration		Oculus Rift vs Touch Haptic	0.609
		Oculus Rift vs Space Mouse	0.072
		Touch Haptic vs Space Mouse	0.212
Scenario B Duration		Oculus Rift vs Touch Haptic	0.103
		Oculus Rift vs Space Mouse	0.003
		Touch Haptic vs Space Mouse	0.080
Scenario C Duration		Oculus Rift vs Touch Haptic	0.052
		Oculus Rift vs Space Mouse	0.638
		Touch Haptic vs Space Mouse	0.064

Figure 6 DISTANCE

Normality tests for Figure 6 DISTANCE
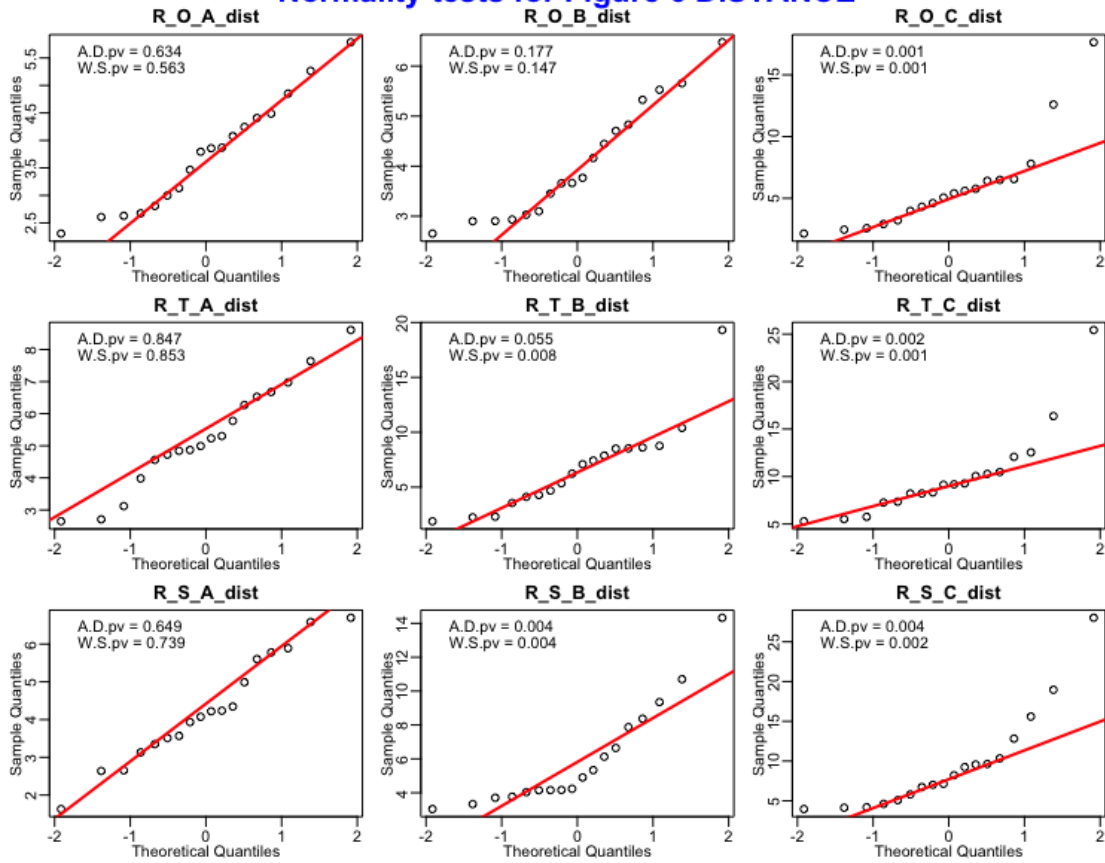
ROBOTIC		Levene's test p-value
Scenario A Distance	Oculus Rift vs Touch Haptic	0.110
	Oculus Rift vs Space Mouse	0.220
	Touch Haptic vs Space Mouse	0.634
Scenario B Distance	Oculus Rift vs Touch Haptic	0.007
	Oculus Rift vs Space Mouse	0.053
	Touch Haptic vs Space Mouse	0.429
Scenario C Distance	Oculus Rift vs Touch Haptic	0.713
	Oculus Rift vs Space Mouse	0.215
	Touch Haptic vs Space Mouse	0.386

Figure 7 DURATION

The normality of each subpopulation has already been tested in Figure 5 (please refer to the previous pages)

	DURATION	Levene's test p-value
Laparoscopic vs Robotic	Oculus Rift Scenario A	0.396
	Oculus Rift Scenario B	0.501
	Oculus Rift Scenario C	0.079
	Touch Haptic Scenario A	0.328
	Touch Haptic Scenario B	0.217
	Touch Haptic Scenario C	0.116
	Space Mouse Scenario A	0.013
	Space Mouse Scenario B	0.097
	Space Mouse Scenario C	0.669

Figure 7 DISTANCE

The normality of each subpopulation has already been tested in Figure 6 (please refer to the previous pages)

	DISTANCE	Levene's test p-value
Laparoscopic vs Robotic	Oculus Rift Scenario A	0.037
	Oculus Rift Scenario B	0.589
	Oculus Rift Scenario C	0.231
	Touch Haptic Scenario A	0.857
	Touch Haptic Scenario B	0.002
	Touch Haptic Scenario C	0.359
	Space Mouse Scenario A	0.190
	Space Mouse Scenario B	0.099
	Space Mouse Scenario C	0.389

Figure 9 DURATION

Normality tests for Figure 9 DURATION
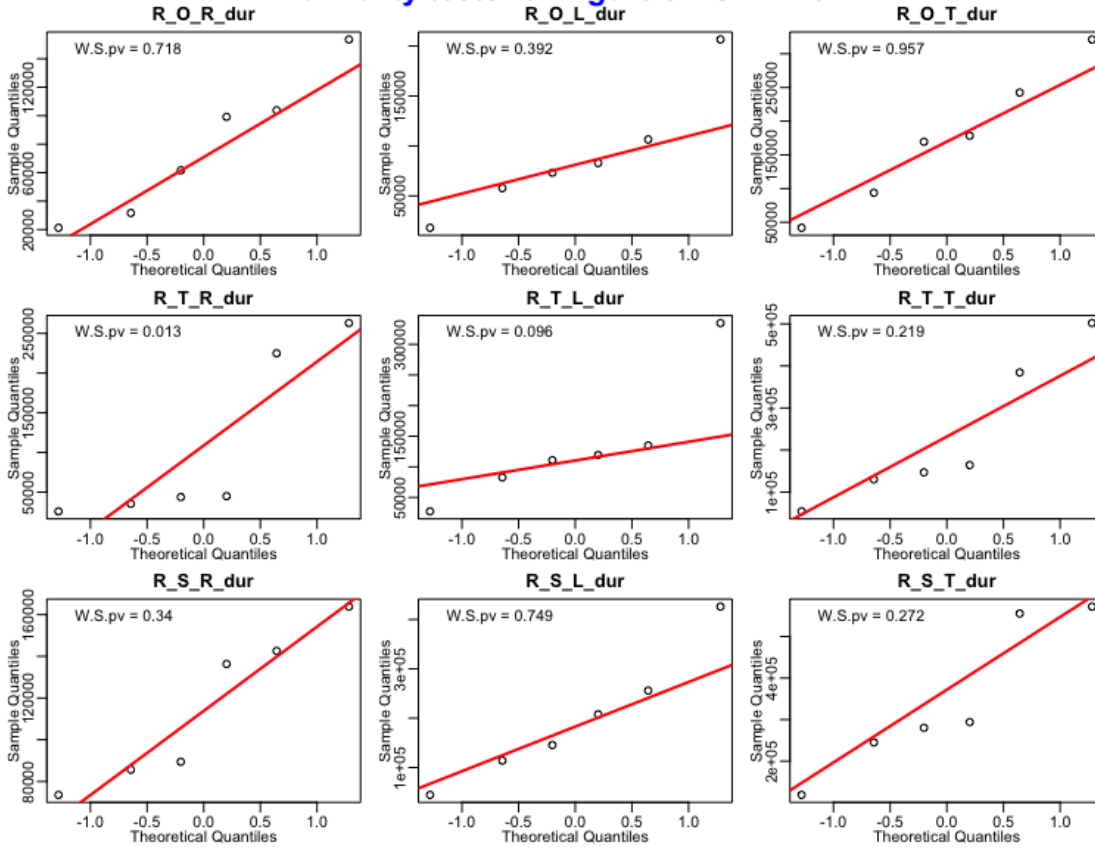
Scenario D - Duration		Levene's test p-value
Right Hand Duration	Oculus Rift vs Touch Haptic	0.477
	Oculus Rift vs Space Mouse	0.466
	Touch Haptic vs Space Mouse	0.366
Left Hand Duration	Oculus Rift vs Touch Haptic	0.618
	Oculus Rift vs Space Mouse	0.179
	Touch Haptic vs Space Mouse	0.468
Total Duration	Oculus Rift vs Touch Haptic	0.467
	Oculus Rift vs Space Mouse	0.351
	Touch Haptic vs Space Mouse	0.902

General Comment:

From the above tests it is evident that in the vast majority the assumptions regarding normality and variance homogeneity are not violated. There are just a few cases (6 out of 45 normality tests and 4 out of 63 variance homogeneity tests) where the p-value of a test (either for normality or variance homogeneity) was below the 0.01 threshold (even though not very far from 0.01) indicating that the null hypothesis was rejected. For all these cases the problem is coming from 1 (or at most 2) outliers that existed in the data, whose removal was sufficient to have p-values that exceed the level of significance. For the above reasons we believe that there is no concern for severe assumption's violation of the t-tests' that were used in the manuscript.